Applied Catalysis A: General 397 (2011) 13–21

Contents lists available at ScienceDirect

Applied Catalysis A: General

journal homepage: www.elsevier.com/locate/apcata

Pillared H-MCM-36 mesoporous and H-MCM-22 microporous materials for conversion of levoglucosan: Influence of varying acidity

M. Käldström[a], N. Kumar[a], T. Heikkilä[b], D.Yu. Murzin[a,*]

[a] Laboratory of Industrial Chemistry and Reaction Engineering, Process Chemistry Centre, Åbo Akademi University, FIN-20500 Åbo/Turku, Finland
[b] Laboratory of Industrial Physics, Department of Physics, University of Turku, FI-20014 Turku, Finland

ARTICLE INFO

Article history:
Received 30 September 2010
Received in revised form 5 January 2011
Accepted 6 January 2011
Available online 12 January 2011

Keywords:
Pillared
Zeolite
MCM-36
Levoglucosan

ABSTRACT

Catalytic transformation of levoglucosan (1-6-anhdyro-β-D-glucopyranose) was carried out in a fixed bed reactor at 573 K over H-MCM-22 and pillared H-MCM-36 with different acidities. The yield of the products, phases and product distribution was influenced mainly by the acidity of the zeolite catalysts. Oxygenated species were the main liquid product, consisting foremost of aldehydes and furfural. The formation of the liquid products was higher over MCM-36 pillared materials than over MCM-22 for all the oxygenated species except acetone. The deactivation due to coking was less severe over the pillared materials compared to the microporous precursor. However, it was possible to successfully regenerate the spent zeolites without changing the structure.

1. Introduction

The transformation of layered zeolite precursors into pillared derivatives was originally driven by the potential of producing a large pore, possibly mesoporous material with high catalytic activity present in the layers.

The molecular sieve MCM-22, belonging to the MWW materials, is a quite unique zeolite in the sense that it can be used as a precursor for synthesizing pillared MCM-36 but also used directly as such in catalytic transformations [1]. MCM-22 contains two different independent pore systems; one of these pore systems is defined by two-dimensional sinusoidal channels, the other consists of large super cages whose inner free diameter, 7.1 Å is defined by 12 T-O species (12-rings) and whose inner height is 18.2 Å [2]. Corma et al. confirmed that the structure of MCM-22 comprises of 10 membered ring (MR) channels together with cavities of larger dimensions (12 MR), both of which can be reached from the external surface [3]. The dimensions of the two types of void systems were furthermore determined to be 5.9 and 7.0 Å, respectively and these cavities are believed to be responsible for the unique catalytic activity of MCM-22, referred to as "surface pocket catalysis" [1,3]. Ravishankar et al. reported that the reason for the precursor to behave like a wide pore (12-MR) catalyst, is thought to be cracks in the crystallites which access the 12-MR cages directly and that the large cages may open out at the external surface wherever there are stacking faults [4]. The adsorption of 2,2-dimethyl butane suggested that pillaring leading to MCM-36 increases accessibility of one kind of pores while others (most likely the 10-member channels) are unaffected [5].

Layered zeolite materials are gaining a lot of interest at the moment and Roth et al. has recently reported a new zeolite entitled EMM-10 based on MWW topology, which is rather similar to MCM-22 microporous material [6]. Corma et al. reported, for the synthesis of MCM-22 zeolite, a requirement in a relatively narrow range of SiO_2/Al_2O_3 ratio compared to other high silica materials [7]. The explanation for this behavior was linked to difficulties in nucleation in the gels. Reported means of partly avoiding this problem were progressive lowering the pH when increasing the ratio and by lowering the synthesis temperature from 423 K to 408 K. Dumitriu et al. showed, however, that a relatively broad range of acidity can be obtained for the MCM-22 type materials by isomorphous substitution of Al, Ga and Fe for silicon in the lattice of the zeolite [8]. The materials were furthermore successfully tested in the gas-phase condensation of isobutylene with formaldehyde, confirming the different properties of the materials.

The synthesis of MCM-36 proceeds through the synthesis of MCM-22 and the subsequent swelling and pillaring of the precursor. The swelling has been successful by addition of 29% cetyltrimethylammonium hydroxide through anion exchange of the concentrated chloride solution [1]. The swelling taking place at high pH is specific by deprotonation of surface silanols with associated disruption of the hydrogen bonds that keep the layers connected to each other. Maheshwari reported that the swelling usually takes place at elevated temperatures (353 K) but that it

* Corresponding author.
E-mail address: dmurzin@abo.fi (D.Yu. Murzin).

0926-860X/$ – see front matter © 2011 Elsevier B.V. All rights reserved.
doi:10.1016/j.apcata.2011.01.008

also can be successful at low temperatures (room temperature) [9]. The difference between the swelling at elevated temperatures compared to room temperature is that in the former case layer atomization along with partial dissolution of the framework silica is achieved, whereas higher crystallinity and well-preserved layer structure is achieved by carrying out the swelling at room temperature [10]. This is shown through X-ray diffraction (XRD) with less broadening of peaks of the material swollen at low temperature compared to the results when the material is swollen at high temperature. Reversibility of the room temperature swelling process was also demonstrated by the same group, which represents a major difference from high-temperature methods that yield irreversibly swollen materials [9]. The reversing process of the swelled material is done by acidification, and the limit of the reversibility behavior has been determined to about 328 K, above this temperature the reversibility was lost due to the partial dissolution of framework silica and destruction of the layered structure.

Pillaring with alumina or magnesia-alumina species has also been investigated yielding mesoporous materials with lower surface area than those pillared with silica [11]. The pillaring procedure in general does not yield mesopores of perfect regular size as for example in the MCM-41 type materials. Instead, the interlayer distances depend upon the process of swelling and formation of the intercalating pillars, i.e. the synthesis conditions. The successful preparation of pillared or delaminated zeolite is confirmed using X-ray diffraction and TEM, which also allow detection of M41S impurities if present in significant amount. MCM-36 complements furthermore the more common and easier to produce M41S materials as a mesoporous catalyst because of high zeolitic activity [12]. Roth et al. presented recently an expanded view unifying the traditional 3-D zeolite frameworks with the layered zeolite structures [13]. They reported that the conventional 3-D frameworks can even be regarded as particular cases of the layers assemblies.

MCM-22 and MCM-36 catalysts have been used in a number of different applications. Iron modified MCM-22 has been shown to be effective in oxidation of benzene with N_2O [14], whereas MCM-36 has for example proven to be a stable, active and selective catalyst in isobutene/2-butene alkylation [15], as well as alkylation of benzene with propylene [16]. Among other reactions m-xylene transformation over the pillared zeolite has been reported [17]. Lipase immobilization on MCM-36 support for acylation of 1-butanol and 1-octanol by vinyl acetate and vinyl stearate as a test reaction has been investigated [18]. MCM-36 additives with mixed alkaline earth aluminum oxide pillars have furthermore been demonstrated to be highly active as additives for the reduction of NO with CO under reaction conditions similar to the oxygen depleted zone of the FCC regenerator [19]. Ni modified MCM-22 and MCM-36 have been used in oligomerization of ethylene [20], and the Ni modified MCM-36 has been shown to perform very well in the oligomers formation. Ti modified MCM-36 has exhibited superior performance compared to Ti-MCM-22 in catalytic activity and selectivity in 1-hexene and propylene epoxidation using H_2O_2 (30%, aqueous) as an oxidant [21].

The conversion of carbohydrates on zeolites has gained a lot of interest recently and has been reported by a number of different research groups [22–25]. In this paper, the influence of mesoporous H-MCM-36 and H-MCM-22 microporous zeolite catalysts on transformation of levoglucosan was investigated, changing also the residence time and by varying the substrate to catalyst ratio between 0.8 and 2.5. The aim with the work was to study the reaction pathways present and products formed in catalytic upgrading of levoglucosan as a means of learning more about cellulose pyrolysis. The monosaccharide levoglucosan (1-6-anhydro-β-D-glycopyranose) is an interesting compound since it is the intermediate through which cellulose decomposes pyrolytically forming lower molecular compounds.

The zeolite and the mesoporous materials synthesized and used in the study were characterized by different physico-chemical techniques such as nitrogen sorption, XRD, SEM and FTIR.

2. Experimental

2.1. Catalyst synthesis and characterization

The Na-MCM-22 microporous molecular sieve with three different acidities was synthesized according to the procedure described elsewhere [26–29] with some modifications. The synthesis of the zeolite was carried out using the following procedure: water and sodium aluminate (Riedel-de Haën, purity ≥95%) was added to sodium hydroxide (Merck, purity ≥99%) and the mixture was stirred for 10 min. After the stirring hexamethyleneimine (Aldrich, purity 99%) and fumed silica (Aldrich purity 99.8%) were added and the blend was stirred for another 20 min. After forming a homogenous phase the mixture was transferred to teflon cups and inserted into autoclaves. The synthesis was carried out at 423 K for 7 days. After completion of synthesis the material was filtered, washed with distilled water to neutral pH, dried at 373 K and calcined at 823 K for 8 h.

MCM-36 zeolite was prepared by swelling the MCM-22 zeolite precursor with organic molecules followed by pillaring with polymeric silica [18]. The synthesis of Na-MCM-36 consisted of three different processes: *swelling*, *pillaring* and *hydrolysis*.

2.1.1. Swelling process

Wet cake of MCM-22 was mixed with cetylmethylammonium chloride solution (25%, Aldrich) and tetrapropyl ammonium hydroxide solution (20%, Aldrich) and the pH was adjusted to 13.5 with NaOH solution. The mixture was then heated and stirred at 373 K for 68 h, and later stirred at room temperature for 4 h. This was followed by washing with distilled water and drying at room temperature.

2.1.2. Pillaring process

Swollen MCM-22 was mixed with TEOS and stirred at 351 K for 25 h. The material was then filtered and dried at room temperature.

2.1.3. Hydrolysis process

Distilled water was added to MCM-36 and the pH was adjusted to 8. The hydrolysis was carried out at 313 K for 6 h. The material was later filtered and dried at room temperature and calcined at 823 K in air.

Na-MCM-22 microporous and Na-MCM-36 mesoporous materials were transformed to NH_4-MCM-22 and NH_4-MCM-36 by ion-exchange using ammonium nitrate solution. H-MCM-22 and H-MCM-36 catalysts were obtained by calcination of NH_4-MCM-22 and NH_4-MCM-36 at 773 K. In the nomenclature given to the H-MCM-22 microporous matererials the numbers 28, 50 and 100 indicate the molar ratio of Si/Al in the framework structure, thus a large number indicates low aluminum content and fewer acid sites. The complete nomenclature of the pillared molecular sieves is hence H-MCM-36-P22–28, H-MCM-36-P22–50 and H-MCM-36-P22–100.

The determination of structure and phase purity of the MCM-22 and MCM-36 molecular sieves was carried out by an X-ray powder diffractometer (Phillips pW 1820) and scanning electron microscopy (SEM). The specific surface area of fresh, used and regenerated H-MCM-22 and H-MCM-36 catalysts was measured by the nitrogen adsorption method (Sorptometer 1900, CarloErba Instruments). The fresh and regenerated catalysts were out gassed at 473 K, whereas the spent catalyst were outgassed at 393 K prior to the measurement and BET equation was used to calculate the specific surface area.

The H-MCM-22 and H-MCM-36 catalysts were regenerated in an oven by calcination at 723 K for 120 min.

The acidity of the synthesized zeolites was measured by infrared spectroscopy (ATI Mattson infinity spectrometer) using pyridine (≥99.5%) as a probe molecule for qualitative and quantitative determination of both Brønsted and Lewis acid sites. The FTIR spectrometer was equipped with an *in situ* cell containing ZnSe windows. The samples were pressed into thin self-supported discs (weight 15–20 mg and radius 0.65 cm). Pyridine was first adsorbed for 30 min at 373 K and then desorbed by evacuation at different temperatures (523, 623 and 723 K) to obtain a distribution of acid site strengths. All spectra were recorded at 373 K with a spectral resolution equal to 2 cm^{-1}. Spectral bands at 1545 and 1450 cm^{-1} were used to identify Brønsted acid sites (BAS) and Lewis acid sites (LAS). The amounts of BAS and LAS were calculated from the intensities of corresponding spectral bands, using the molar extinction coefficients reported by Emeis [30].

The Si/Al ratio of the micro-and mesoporous materials was determined by laser ablation-ICP-MS. The laser ablation instrument was of the type UP-213, from New Wave Research, Merchantek System. The ICP-MS instrument was a PerkinElmer Sciex, ICP Mass Spectrometer of the type Elan 6100 DRC+.

2.2. Experimental set-up for catalyst testing

Transformation of levoglucosan (1-6-β-D-glucopyranose) in gas phase at atmospheric pressure was chosen as the model test reaction. The catalyst testing equipment consisted of a quartz mini reactor, an oven, an evaporator and a condenser.

Levoglucosan (Aldrich, purity 99%) was dissolved in deionised water to make a 1% solution, which was fed through an evaporator operating at 573 K into the quartz fixed bed reactor with an inner diameter of 9 mm. This quartz mini reactor was packed with the zeolite catalyst (150–250 μm) and inserted into the oven. In order to get a narrow particle size range for the zeolite catalyst, pellets of the zeolite powder were pressed and thereafter crushed and sieved. The temperature of the catalyst bed was measured using a thermocouple and the temperature of the reactor was monitored with a temperature controller. Nitrogen gas with a flow of 58.1 ml/min was used as a carrier gas. The products were cooled down with a condenser containing glycol solution at 268 K and collected in a flask.

The feed of levoglucosan was adjusted to 4 ml/h. The catalyst testing and the evaporation of levoglucosan were carried out at temperature 673 K and the catalyst amount was 0.08, 0.125 and 0.25 g. The catalyst bed height was measured before the experiments giving a possibility to calculate the weight hourly space velocity (WHSV) and residence time. In every experiment the levoglucosan solution was fed into the reactor for 5 h which gave a total volume of 20 ml liquid and 200 mg of pure levoglucosan. After each experiment the total amount of liquid was weighted. The following day the evaporator was thoroughly washed by passing water through it to rinse out levoglucosan that was left and could affect the mass balance. The water used for washing was always weighted and analyzed for determining the amount of levoglucosan.

2.3. Product analysis

Liquid samples were analyzed with HPLC and the volatiles with a gas chromatograph connected to a mass-spectrometer (GC–MS).

2.3.1. Total organic carbon

The total organic carbon (TOC) was determined of the liquid phase after each experiment. The analyses were performed using a Total organic carbon analyzer, TOC-V CSN, delivered by Shimadzu Corporation.

2.3.2. GC-MS-solid phase micro extraction

The volatile compounds were analyzed with GC/MS and headspace solid phase micro extraction (SPME). 2 ml of the solution containing the reaction products were transferred into a small 4 ml flask equipped with a rubber cap. The sample flask was heated to 320 K. The needle with the fibre was penetrated through the cap into the bottle and the fibre was exposed to the headspace of the sample for 30 min. The fibre used for extraction was coated with carboxen/polymethylsiloxane (CAR/PDMS). The components were enriched on the surface when equilibria were reached between the headspace and the fibre, thereafter the syringe was injected into the GC–MS for analysis. The inlet chamber was set on 543 K, where the absorbed and adsorbed analytes were thermally desorbed in the hot injector of the gas chromatograph. The GC–MS was equipped with a capillary column (DB-Petro 50 m × 0.2 mm × 0.5 μm). The following temperature program was used: dwelling for 10 min at 313 K, heating 0.9 K/min to 348 K followed by heating 1.1 K/min to 393 K, heating 10 K/min to 473 K and dwelling at 473 K for 20 min.

2.3.3. GC–MS–MTBE extraction

Since the mixture of formed products was quite complex, the product analysis was challenging and the water phase could not directly be injected into the GC–MS, extraction with MTBE was utilized as an additional means to detect any product formed in large amount and not yet determined. The components in the liquid phase were therefore extracted with the organic solvent and analyzed with GC–MS. 0.5 ml of both the sample and MTBE were mixed in a tube to extract the polar compounds into the MTBE-phase. The organic solvent was removed after extraction from the tube and inserted into GC-vials and analyzed with GC–MS. The same column was used as in the solid phase micro extraction and the temperature program used was as follows: dwelling for 1 min at 313 K, heating 6 K/min to 553 K and dwelling for 5 min.

2.3.4. High performance liquid chromatography (HPLC)

The products from the test reaction with levoglucosan were also analyzed with HPLC equipped with an acid Aminex HPX-87C column connected to a refractive index (RI) detector. Diluted calcium sulphate solution ($CaSO_4$, 1.2 mM was used as a mobile phase. The flow was 0.4 ml/min and the temperature was set to 353 K. The samples were injected into the HPLC directly after the experiments without any pretreatment other than filtering. Varying concentrations of different standards were made and analyzed with the HPLC. The standards were purchased from Aldrich or Fluka and had a purity of ≥99%. The HPLC was calibrated with the different standards and upon the results calibration curves were drawn which made it possible to calculate the molar yields of the achieved products. HPLC was also used to calculate the conversion rate of levoglucosan.

2.3.5. Coke analysis

2.5 ml of hydrofluoric acid (HFA) (Merck 40%) was added to 0.15 g of zeolite for dissolving for 1 h. The mixture was agitated between short time intervals. 10 ml of dichloromethane was added to the dissolved mixture. The soluble particles were extracted for 24 h and the non-soluble components were recovered. HFA and dichloromethane formed two phases which were separated with an extraction funnel. The dichloromethane phase was filtrated and analyzed with GC–MS. The filter paper was dried and weighted prior to, and after filtering to determine the total amount of non-dissolvable coke. The following temperature program was used: dwelling for 10 min at 373 K, heating 277 K/min to 493 K followed by heating 275 K/min to 573 and dwelling at 573 K for 20 min.

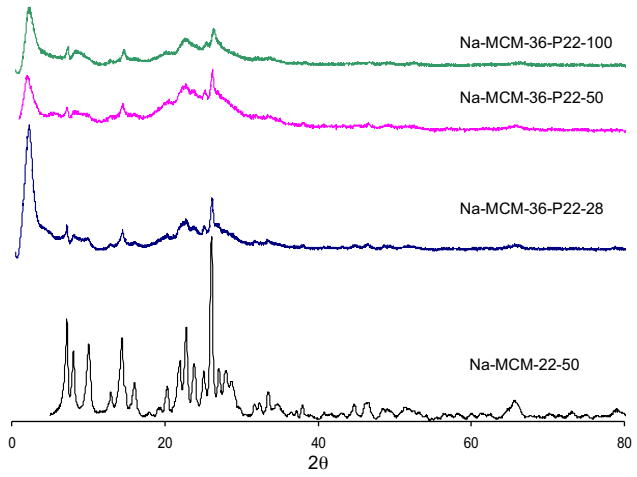

Fig. 1. X-ray powder diffraction pattern of Na-MCM-22–50 microporous material along with Na-MCM-36-P22–28, Na-MCM-36-P22–50 and Na-MCM-36-P22–100 mesoporous material.

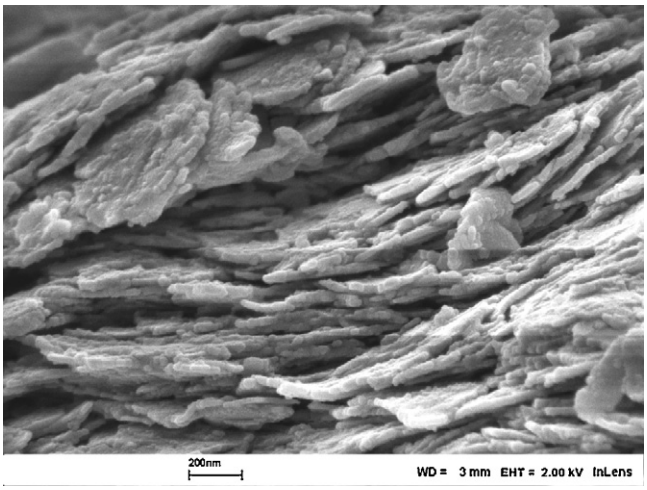

Fig. 2. Scanning electron micrograph of Na-MCM-36-P22–50 mesoporous material.

2.3.6. TGA

The amount of coke formed on the precursor H-MCM-22–50 and the pillared H-MCM-36-P22–50 were determined by thermogravimetrical analysis (TGA) using a Cahn D-200 digital recording balance under the flow of synthetic air. The following temperature program for the oven was used: heating 2 K/min from 298 K to 873 K and dwelling at 873 K for 180 min.

3. Results and discussion

3.1. Catalyst characterization results

XRD patterns of Na-MCM-22 microporous and Na-MCM-36 mesoporous materials were similar to those reported in the literature, indicating phase purity of the synthesized materials. The XRD patterns of all the materials are given in Fig. 1 and scanning electron micrograph of Na-MCM-36-P22–50 is given in Fig. 2. The XRD of the MCM-36-P22–100 mesoporous material is somewhat less crystalline then the XRDs of the other pillared catalysts. Furthermore a very faint irregularity was detected at 4.7° which could indicate a trace impurity in the sample. The sample bulk was, however, identified as MCM-36.

The Brønsted and Lewis acidities of the studied H-MCM-22 and H-MCM-36 catalysts, as determined by pyridine adsorption (FTIR), are presented in Table 1. There is a substantial difference in the acidity between the catalysts. The difference is especially substantial when comparing the Brønsted acid sites of the two materials.

Compared to other mesoporous materials such as MCM-41 and MCM-48, MCM-36 exhibits considerably higher acidity. There is always a decrease in the Brønsted acidity during the synthesis of MCM-36 from MCM-22 due to the delamination and pillarization. This is a fact since the number of acid sites at the actual external surface is diminished by between 17–82%, as confirmed by acidity measurements with ammonia and pyridine as probe molecules [15,31]. The Lewis acid sites have been reported to both increase and decrease during the formation of the pillared mesoporous material [17,31].

The difference in the amount of Brønsted acid sites between H-MCM-36-P22–50 and its precursor H-MCM-22–50 is a factor of 3.6 in favour of the latter, which means that only 27% of the Brønsted sites are left after pillaring. The difference between the amount of Lewis sites is much smaller. The ratio in Lewis acidity between the same catalysts is 1.2 in favour of the precursor. The acidity, both Brønsted and Lewis, decreases as expected in the following order H-MCM-36-P22–28 > H-MCM-36-P22–50 > H-MCM-36-P22–100.

The actual Si/Al ratio of the different catalysts as determined by laser ablation-ICP-MS is reported in Table 2. The ratio for the microporous material was rather low since the theoretical value was expected to be 50. The H-MCM-22–50 microporous material was, however, considerably more acidic then synthesized H-MCM-22–30 catalysts [32]. This could indicate that the reason for the low value for the H-MCM-22–50 microporous material could originate from some imprecision in the calibration of the analysis equipment.

The surface area for the fresh microporous MCM-22 and mesoporous MCM-36 was measured with nitrogen adsorption and calculated with BET equations (Table 3). With silica as the pillaring material, the surface area of MCM-36 has been reported to be between 1.5 and 3 times larger than that of MCM-22 [15,18]. The surface area of successfully synthesized MCM-22 has been reported to vary between 343 [16] and 560 m^2/g [9], whereas the surface area of MCM-36 catalysts has been declared to vary greatly, between 535

Table 2
Si/Al ratio as determined by LA-ICP-MS.

Catalyst	Si/Al ratio
H-MCM-22–50	35
H-MCM-36-P22–28	47
H-MCM-36-P22–50	65
H-MCM-36-P22–100	92

Table 1
Lewis and Brønsted acid sites of H-MCM-22 and H-MCM-36 catalysts.

	Brønsted acid sites (μmol/g)			Lewis acid sites (μmol/g)		
Catalyst	523 K	623 K	723 K	523 K	623 K	723 K
H-MCM-22–50	208	191	141	47	19	5
H-MCM-36-P22–28	87	70	44	61	32	6
H-MCM-36-P22–50	57	48	23	40	23	5
H-MCM-36-P22–100	36	32	12	31	15	3

Table 3
Surface area of fresh and used H-MCM-22 and H-MCM-36 catalysts.

Catalyst	Surface area (m^2/g), BET				Pore specific volume (cm^3/g)
	Amount (g)	Fresh	Used	Regenerated	
H-MCM-22–50	0.08	387	7	350	0.20
	0.125		47		
	0.25		97		
H-MCM-36-P22–28	0.08	513	85	520	0.70
	0.125		174		
	0.25		204		
H-MCM-36-P22–50	0.08	560	102	560	0.57
	0.125		180		
	0.25		273		
H-MCM-36-P22–100	0.08	618	331	611	0.76
	0.125		274		
	0.25		378		

[17] and 934 m^2/g [9]. This indicates that for the synthesis of MCM-36 to be successful the surface area should exceed 500 m^2/g. The specific pore volume was also determined and the volume of the pores was about three times larger for the mesoporous material compared to the microporous precursor, which also indicates the successful pillaring (Table 3).

3.1.1. Characterization of the used catalysts

The surface area of spent and regenerated catalysts was also measured with nitrogen adsorption and calculated with BET equation (Table 3). The decrease in surface area was inversely related to the amount of catalyst as expected. The decrease in surface area was more severe in the case of MCM-22 than in the case of the different MCM-36 samples. It seemed furthermore that H-MCM-36-P22–100 was least affected by the deactivation due to coke formation of the different MCM-36 catalysts. It was possible to successfully regain the surface area of all the catalysts by regeneration in air at 723 K for 2 h (Table 3). Furthermore recent studies of mesoporous materials in the same reactor system have shown full recovery of the acidic sites as well as of the catalytic activity by regeneration in air at 723 K [33]. Differences in deactivation and coke formation between MCM-22 and MCM-36 have also been reported by other research groups. Corma et al. reported that the amount of coke was higher on MCM-36 than over MCM-22 in the conversion of olefins to paraffins [31]. This was thought to be due to the much lower catalytic activity of MCM-36, which was assumed to be responsible for the important contribution of the nonselective thermal cracking to the global conversion and selectivities observed. Deactivation has, however, also been shown to be much slower over MCM-36 than over MCM-22 [1], in the transformation of m-xylene, which indicates that coking and deactivation of MCM-36 takes place not only in the supercages but also in part of the supermicropores created by pillaring [17].

3.2. Product characterization results

3.2.1. Product distribution between the gas and liquid phases

The product distribution between phases after condensation of gases was evaluated through measuring total amount of carbon. The results shown in Fig. 3 report the yield of total organic carbon in the liquid phase compared to the total amount of carbon inserted into the system with the introduction of levoglucosan. The least total organic carbon was found in the liquid phase from the transformation of levoglucosan over MCM-22 catalyst followed by H-MCM-36-P22–28, whereas the amounts detected in the liquid phase from transformations over H-MCM-36-P22–50 and H-MCM-36-P22–100 mesoporous materials were rather similar. The amount of total carbon which was condensed decreased with increasing residence time indicating larger generation of gases due to consecutive reactions.

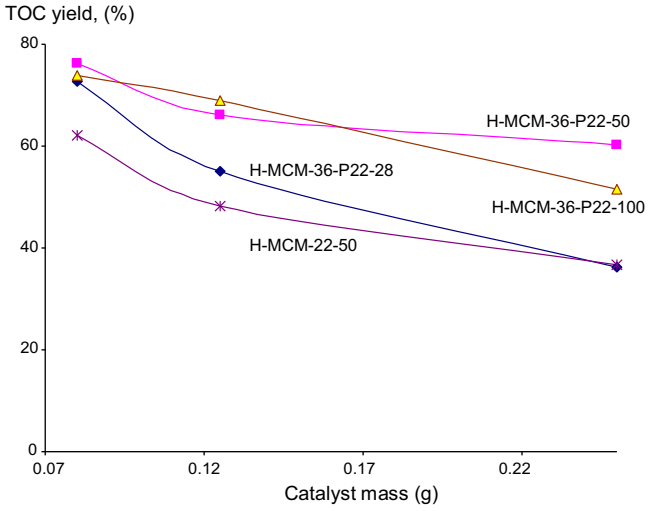

Fig. 3. Total amount of organic carbon detected in the condensed phase from catalytic transformations over microporous H-MCM-22–50 and H-MCM-36-P22–28, H-MCM-36-P22–50 and H-MCM-36-P22–100 mesoporous materials.

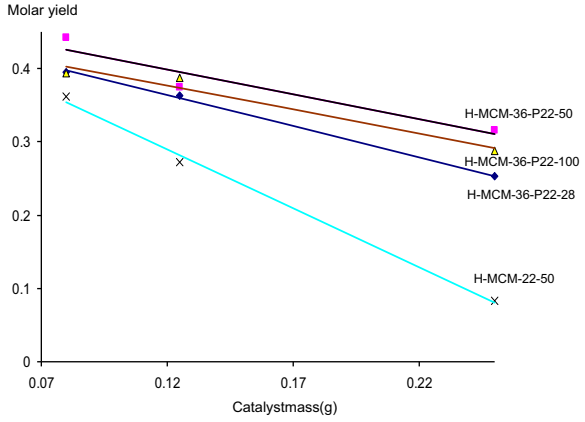

Fig. 4. Generation of glycolaldehyde over H-MCM-22–50, H-MCM-36-P22–28, H-MCM-36-P22–50 and H-MCM-36-P22–100 catalysts.

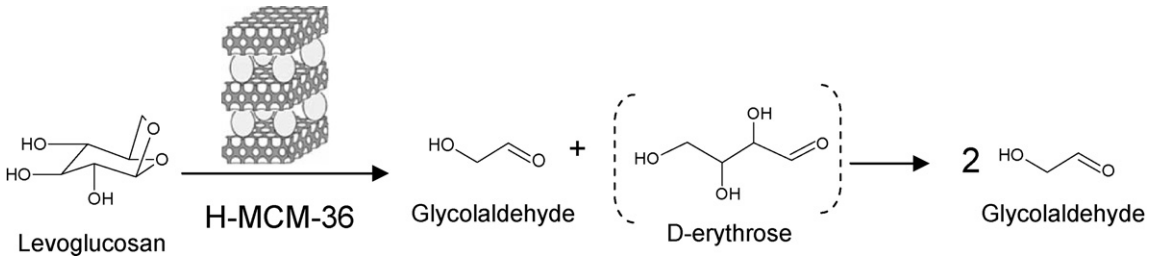

Fig. 5. Reaction scheme for the formation of glycolaldehyde from levoglucosan based on experimental results and literature [1,28].

3.2.2. Products/selectivity

The conversion of levoglucosan was 100% with all the catalysts. The product distribution varied, however, between different catalysts and residence time.

3.2.2.1. Formation of glycolaldehyde. Formation of the major product, glycolaldehyde, was the highest over H-MCM-36-P22–50 catalyst followed by H-MCM-P22–100 and H-MCM-P22–28 (Fig. 4). The formation is reported as molar yield, which refers to the total amount of moles of formed glycolaldehyde compared to the total amount of input levoglucosan. All the three forms of MCM-36 showed higher amounts of glycolaldehyde than MCM-22 allowing to conclude that the pillaring process was favorable in the formation of glycolaldehyde from levoglucosan. Srokol et al. reported that especially base catalyzed reactions of D-glucose results in the formation of glycolaldehyde, claming that important hydrothermal reactions of glucose and other C6 sugars starts with a retroaldol condensation to form glycolaldehyde [34]. They reported furthermore that the second product in the reaction should be a C4 sugar such as D-erythrose which was proposed to further also react into glycolaldehyde (Fig. 5). However, as in the experiments performed by Srokol et al., no D-erythrose was detected in the transformation of levoglucosan, indicating that the consequent reaction into glycolaldehyde is very fast.

The formation of glycolaldehyde over the pillared catalyst was higher throughout the whole experiment compared to the microporous precursor (Fig. 6). The values are reported as yield, comparing the concentration of formed glycolaldehyde with the concentration of levoglucosan input solution. Starting from a similar value as the production over H-MCM-22–50 the formation over the mesoporous catalyst increased fast and was detected at elevated levels during the whole experiments compared to the former catalyst. While the generation of glycolaldehyde over H-MCM-36-P22–50 went through a maximum after 120 min, and thereafter started to decline because of catalyst deactivation due to coke formation, the generation over the microporous precursor increased during the whole experiment.

Since acidity is crucial for the formation of the low molecular products such as glycolaldehyde, one explanation for the product increase over H-MCM-22–50 is that the material is initially too active leading to consecutive products forming gases such as carbon monoxide and carbon dioxide. The production of glycolaldehyde

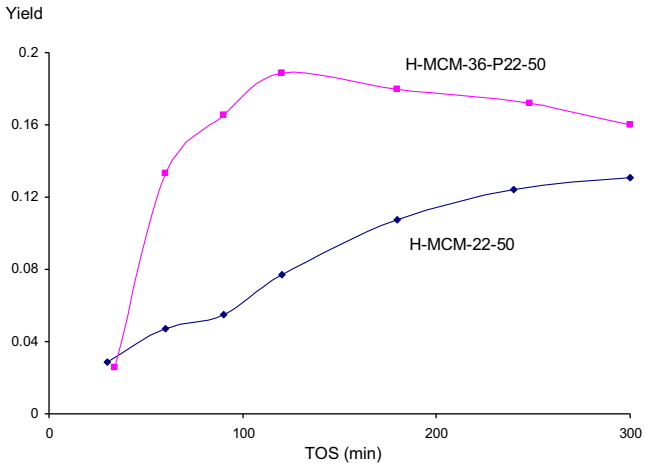

Fig. 6. TOS generation of glycolaldehyde over H-MCM-22–50 and H-MCM-36-P22–50 catalysts at residence times of 0.23 and 0.3 s respectively.

Table 4
Molar yields of minor products detected in the transformation of levoglucosan over MCM-22 and MCM-36 catalysts.

Products, H-MCM-22–50	Residence time (s)		
	0.13	0.23	0.46
Acetic acid	0.01	0.01	–
Glyoxal	0.01	–	–
Formaldehyde	0.11	0.1	–
Acetaldehyde	0.16	0.13	0.08
Acetone	0.17	0.06	0.06
Furfuryl alcohol	–	–	–
5-Hydroxymethyl furfural	0.04	0.02	0.01
Furfural	0.7	0.07	0.01
Products, H-MCM-36-P22–28	**Residence time (s)**		
	0.20	0.30	0.56
Acetic acid	–	–	0.01
Glyoxal	0.01	–	0.01
Formaldehyde	0.14	0.16	0.12
Acetaldehyde	0.33	0.32	0.23
Acetone	0.05	0.1	0.06
Furfuryl alcohol	0.01	0.01	0.01
5-Hydroxymethylfurfural	0.02	0.01	–
Furfural	0.09	0.09	0.04
Products, H-MCM-36-P22–50	**Residence time (s)**		
	0.20	0.30	0.56
Acetic acid	–	0.02	0.01
Glyoxal	–	0.01	0.01
Formaldehyde	0.16	0.1	0.1
Acetaldehyde	0.25	0.17	0.17
Acetone	0.09	0.05	0.04
Furfuryl alcohol	–	–	–
5-Hydroxymethylfurfural	0.06	0.06	0.06
Furfural	0.1	0.06	0.05
Products, H-MCM-36-P22–100	**Residence time (s)**		
	0.20	0.30	0.56
Acetic acid	–	–	–
Glyoxal	0.02	0.01	–
Formaldehyde	0.09	0.14	0.14
Acetaldehyde	0.14	0.12	0.13
Acetone	0.06	0.06	0.06
Furfuryl alcohol	–	–	0.01
5-Hydroxymethylfurfural	0.04	0.05	0.01
Furfural	0.07	0.08	0.07

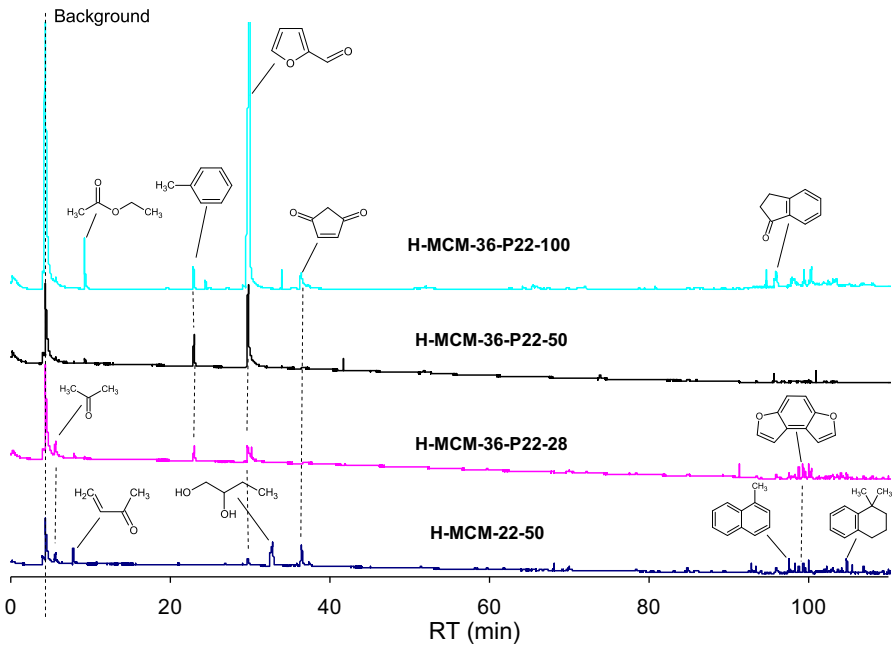

Fig. 7. GC–MS spectra combined with SPME for product mixture obtained over 0.25 g of H-MCM-22 and three H-MCM-36 catalysts with different acidities.

is thereby benefitted by the decrease in acidity originating from catalyst deactivation due to coke formation. The other detected products, shown in Table 4, and determined by comparing the retention times with standard solutions, consisted of different aldehydes, furfurals, acetone and acetic acid.

3.2.2.2. Formation of furfurals. Signals with similar retention times as those of furfural, furfuryl alcohol and 5-hydroxy methyl furfural (5HMF) were detected with HPLC when analyzing the liquid samples (Table 4). Furfural was the most abundant of the detected furfural compounds. At a low residence time it was found to be formed at the same extent over all catalysts. However, at the longest residence time (0.25 g of catalyst) some differences between the different molecular sieves were detectable, i.e. furfural generation increased in the following order H-MCM-22–50 < H-MCM-36-P22–28 < H-MCM-36-P22–50 < H-MCM-36-P22–100. 5HMF and furfuryl alcohol were formed to lower extent. Most 5HMF was detected with H-MCM-36-P22–50 followed by H-MCM-36P22–100.

3.2.2.3. Formation of acetaldehyde and formaldehyde. Formation of formaldehyde was higher over all MCM-36 mesoporous materials compared to MCM-22 (Table 4). The amount of it decreased with increasing residence time over MCM-22, whereas it was not possible to establish any trend for the mesoporous materials. Generation of acetaldehyde was also higher for MCM-36 than in case of MCM-22. The amount formed decreased with increasing residence time for all the tested catalysts except H-MCM-36-P22-100, for which the yield remained at a constant level even though the residence time changed. As for the pillared materials the following order was observed in the formation of acetaldehyde: H-MCM-36-P22-28 > H-MCM-36-P22-50 > H-MCM-36-P22-100, which was in line with acidity decrease.

3.2.3. SPME combined with GC–MS

The main volatile products detectable with HPLC were also observed with GC–MS (Fig. 7). The largest peak corresponding to furfural, increased in the order H-MCM-22–50 < H-MCM-36-P22–28 < H-MCM-36-P22–50 < H-MCM-36-P22–100, in line with HPLC analysis.

Table 5
Increase of reactor weight due to tar and coke formation over H-MCM-22–50 and H-MCM-36 catalysts.

Catalyst	Mass (mg)	Reactor weight increase (mg)	Yield (wt%)
H-MCM-22–50	80	15	8
	125	21	11
	250	23	12
H-MCM-36-P22–28	80	16	8
	125	22	11
	250	29	14
H-MCM-36-P22–50	80	18	9
	125	19	10
	250	20	10
H-MCM-36-P22–100	80	19	10
	125	9	4
	250	16	8

Other detected products were acetone, ethyl acetate, 3-buten-2-one, toluene, 1,2-butanediol, 4-cyclopentene-1,3-dione, 1-indanone, benzo[1,2-b;4,3-b]difuran and different naphthalenes. 3-buten-2-one and 1,2-butanediol were only seen over H-MCM-22–50, whereas toluene was only observed over the mesoporous materials.

3.2.3.1. Extraction with MTBE. The products detected by extraction were furfural, ethanol, 2-cyclopentene-1-one, 5-methyl-(2H)-furanone, 4-cyclopentene-1,3-dione, furfuryl alcohol and 5-methyl furfural. Furfural was by far formed to the largest extent, based on compared peak areas, which indicates that the other products were formed in only minor quantities.

3.2.3.2. Formation of tar. It should be mentioned that there was also some formation of tar on the inside of the reactor walls. The total weight of formed tar and coke on the catalyst was determined by weighing the dry reactor prior to, and after the experiments (Table 5). The formed coke and tar varied between 9 and 29 mg, resulting in a total coke and tar yield that substituted between 5 and 15% of the input levoglucosan. The tar and coke formation increased with increasing catalyst amount over H-MCM-22–50, H-MCM-36-

Table 6
Mass balance calculated for microporous H-MCM-22–50 and mesoporous H-MCM-36-P22–50.

Residence time (s)	Levoglucosan left in prereactor (mg)	Reactor weight increase		TOC (mg)	Total mass (mg)	Mass balance (%)
		Total (mg)	Coke (mg)			
H-MCM-22–50						
0.13	9	15	11	124	148	74
0.23	8	21	18	96	125	63
0.46	8	23	(27)	74	105	53
H-MCM-36-P22–50						
0.2	7	18	10	152	177	89
0.3	8	19	15	132	159	80
0.56	10	20	(23)	120	150	75

P22–28 and H-MCM-36-P22–50 while no clear trend was visible with H-MCM-36-P22–100.

3.3. Coke characterization results

The total amount of coke formed and analyzed with TGA was larger over microporous H-MCM-22–50 than over pillared H-MCM-36-P22–50 catalyst (Fig. 8). The products detected from the coke analysis after dissolving the zeolites were mainly long hydrocarbon chains like hexadecane, heptadecane, 1-heptadecene, octadecane, 1-octadecene and 1-nonadecane. Aho et al. have previously also reported about linear alkanes and alkenes extracted from coke on mesoporous materials used in catalytic transformations of cellulose [35]. The percentage of insoluble coke for the different catalysts is shown in Table 7. The amount of insoluble coke formed on H-MCM-22 was two-threefold compared to the amount formed on the pillared zeolites.

3.4. Mass balance

The mass balance was calculated based on the increase in weight of the reactor, the amount of left-over levoglucosan in the prereactor and the measured TOC on the liquid phase (Table 6). The sum of the masses of the different products was compared with the total amount of input levoglucosan (200 mg). The values for TOC were determined by dividing the measured values of the total amount of organic carbon detected in the liquid with the total amount of carbon in the input levoglucosan. This ratio was then multiplied with the input levoglucosan (200 mg). The total amount of coke was calculated based on TGA measurements, whereas the amount of left-over levoglucosan in the prereactor was determined by analyzing the water used for rinsing it with HPLC. The reason for the increase in the weight of the reactor was due to coke formation on the catalyst as well as tar formation on the reactor wall beneath the catalyst bed. The values for the formation of coke on the two largest amounts of catalyst (0.25 g, residence time 0.46 and 0.56) are probably too large and are therefore shown in parenthesis, since the numbers are even larger than the total reactor weight increase. The values for the amount of coke were calculated by taking the percentage of the catalysts being coked given by TGA (Fig. 8) for the different amount of catalysts, multiplied with the fresh total catalyst mass. One explanation for the high values could be that the catalyst was not evenly deactivated, being more coked on the top of the bed, and that this part was used in the analysis with TGA. When comparing the values for the insoluble coke (Table 7) with the values based on the TGA analysis one can furthermore see that the values for insoluble coke seem too large which indicates that some zeolite particles most probably were left non-dissolvable, despite treatment with HF, and thereby influencing the weight. The error should, however, be similar for all the catalysts since they were treated in a similar manner during analysis, which means that one can conclude that the amount of non-dissolvable coke was substantially larger over microporous MCM-22 than MCM-36 mesoporous material. The mass balance was closest to being complete with 0.08 g of pillared MCM-36-P22–50 (residence time 0.2 s) indicating that only a small part was lost as non-condensable gases. With increasing residence time the value for the mass balance decreased, indicating higher formation of gases. Microporous MCM-22–50 being more acidic than mesoporous MCM-36-P22–50 formed more gases, which can be seen as lower values compared to the corresponding amounts of the pillared catalyst used.

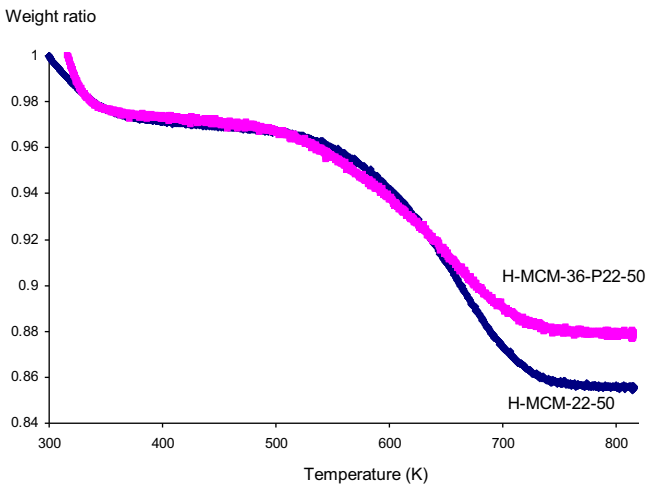

Fig. 8. TGA of 0.25 g of spent H-MCM-22–50 and H-MCM-36-P22–50 catalyst.

Table 7
Formation of insoluble coke over the MCM-22 and MCM-36 catalysts.

Zeolites	Insoluble coke of total catalyst mass (wt%)
H-MCM-22	28
H-MCM-36-P22–28	14
H-MCM-36-P22–50	6
H-MCM-36-P22–100	11

4. Conclusions

The catalytic activity of H-MCM-22 and H-MCM-36 catalysts was investigated in the conversion of levoglucosan at 573 K. Thermal transformations were negligible. The yields of the main and minor products, different oxygenated species (glycolaldehyde, formaldehyde, acetaldehyde, furfural, 5-methyl furfural, acetic acid), varied depending on residence time. Aldehydes were the predominant products followed by different furfural species. The pore sizes of the used materials are all larger than the cross section of levoglucosan 4.2 Å × 5.3 Å [36] as well as the cross sections

of the formed products. This means that the shape selectivity most probably did not have a large effect on the product distribution.

A mass balance excluding the non-condensable gases and comparing transformations over microporous H-MCM-22–50 and mesoporous H-MCM-36-P22–50 was calculated. The balance was the most complete with transformations over H-MCM-36-P22–50 mesoporous material and low residence time. At longer residence times the mass balance was less complete indicating that there is an increase in the formation of gases (CO_2, CO). There was also a significant difference in the formed products between H-MCM-22 and H-MCM-36 catalysts. The former one yielded lower amounts for all the main liquid products except acetone. H-MCM-22–50 is much more acidic than H-MCM-36 catalyst, and thus more active, thereby splitting most of the bonds in levoglucosan into CO_2 and CO. The degree of deactivation of the tested catalyst was quite severe, being more significant over MCM-22 than over the pillared catalysts. It was, however, possible to regenerate the catalysts and regain the surface area.

Acknowledgement

This work is part of the activities at the Åbo Akademi Process Chemistry Centre within the Finnish Centre of Excellence Programme (2000–2011) by the Academy of Finland. L. Österholm is acknowledged for the TOC analysis and Paul Ek is acknowledged for the laser ablation-ICP-MS analysis.

References

[1] W.J. Roth, in: J. Čejka, H. van Bekkum, A. Corma, F. Schüth (Eds.), Introduction to Zeolite Science and Practice, 3rd revised edition, Elsevier B.V., 2007, pp. 221–239.
[2] M.E. Leonowicz, J.A. Lawton, S.L. Lawton, M.K. Rubin, Science 264 (1994) 1910–1913.
[3] A. Corma, C. Corell, J. Pérez-Pariete, J.M. Guil, R. Guil-López, S. Nicolopoulos, J. Gonzalez Calbet, M. Vallet-Regi, Zeolites 16 (1996) 7–14.
[4] R. Ravishankar, D. Bhattacharya, N.E. Jacob, S. Sivasanker, Micropor. Mater. 4 (1995) 83–93.
[5] W.J. Roth, C.T. Kresge, J.C. Vartuli, M.E. Leonowicz, A.S. Fung, S.B. McCullen, in: H.K. Beyer, H.G. Karge, I. Kiricsi, J.B. Nagy (Eds.), Studies in Surface Science and Catalysis, vol. 94, 1995, pp. 301–307.
[6] W.J. Roth, D.L. Dorset, G.J. Kennedy, Micropor. Mesopor. Mater. (2010), doi:10.1016/j.micromeso.2010.10.052.
[7] A Corma, C. Corell, J. Perez-Pariente, Zeolites 15 (1995) 2–8.
[8] E. Dumitriu, V. Hulea, I. Fechete, A. Aurox, B. Dargoi, C. Guimon, Prog. Catal. 12 (2003) 47–53.
[9] S. Maheshwari, E. Jordan, S. Kumar, F.S. Bates, R.L. Penn, D.F. Shantz, M. Tsapatsis, J. Am. Chem. Soc. 130 (2008) 1507–1516.
[10] S. Maheshwari, C. Martinez, M.T. Portilla, F.J. Llopis, A. Corma, M. Tsapatsis, J. Catal. 272 (2010) 298–308.
[11] J.-O. Barth, J. Kornatowski, J.A. Lercher, J. Mater. Chem. 12 (2002) 369–373.
[12] W.J. Roth, J.C. Vartuli, C.T. Kresge, in: A. Sayari, al. et (Eds.), Studies in Surface Science and Catalysis, vol. 129, 2000, pp. 501–508.
[13] W.J. Roth, D.L. Dorset, Micropor. Mesopor. Mater (2010), doi:10.1016/j.micromeso.2010.11.007.
[14] D. Meloni, R. Monaci, E. Rombi, C. Guimon, H. Martinez, I. Fechete, E. Dumitru, in: R. Aiello, G. Giordano, F. Testa (Eds.), Studies in Surface Science and Catalsysis, vol. 142, Elsevier Science, 2002, pp. 167–174.
[15] Y.J. He, G.S. Nivarthy, F. Eder, K. Seshan, J.A. Lercher, Micropor. Mesopor. Mater. 25 (1998) 207–224.
[16] Y. Zhang, H. Xing, P. Yang, P. Wu, M. Jia, J. Sun, T. Wu, React. Kinet. Catal. Lett. 90 (2007) 45–52.
[17] S. Laforge, P. Ayrault, D. Martin, M. Guisnet, Appl. Catal. 279 (2005) 79–88.
[18] E. Dumitiru, F. Secundo, J. Patarin, I. Fechete, J. Mol. Catal. B: Enzym. 22 (2003) 119–133.
[19] J.-O. Barth, A. Jentys, E.F. Ilopoulou, I.A. Vasalos, J.A. Lercher, J. Catal. 227 (2004) 117–129.
[20] M. Lallemand, O.A. Rusu, E. Dumitriu, A. Finiels, F. Fajula, V. Hulea, Appl. Catal. 338 (2008) 37–43.
[21] S.-Y. Kim, H.-J. Ban, W.-S. Ahn, Catal. Lett. 113 (February (3–4)) (2007).
[22] Y.-C. Lin, G.W. Huber, Energy Environ. Sci. 2 (2009) 68–80.
[23] J.J. Bozell, G.R. Petersen, Green Chem. 12 (2010) 539–554.
[24] P. Mäki-Arvela, B. Holmbom, T. Salmi, D. Yu Murzin, in: A.T. Bell, K. Klier (Eds.), Catalysis Reviews, Taylor & Francis Group, 2007, pp. 197–340.
[25] C. Perego, A. Bosetti, Micropor. Mesopor. Mater. (2010), doi:10.1016/j.micromeso.2010.11.007.
[26] S.L. Lawton, M.E. Leowicz, R.D. Partridge, P. Chu, M.K. Rubin, Micropor Mesopor. Mater. 23 (1998) 109–117.
[27] C.T. Kresge, M.E. Leonowicz, W.J. Roth, J.C. Vartuli, US Patent 5,098,684 (1992).
[28] M.A. Asensi, A. Corma, A.J. Martínez, Catalysis 158 (1996) 561–569.
[29] A. Corma, C. Corell, J. Perez, Zeolites 15 (1995) 2–8.
[30] C.A. Emeis, J. Catal. 143 (1993) 347–354.
[31] A. Corma, V. Fornes, J. Martinez-triguero, S.B. Pergher, J. Catal. 186 (1999) 57–63.
[32] M. Käldström, N. Kumar, T. Heikkilä, M. Tiitta, T. Salmi, D. Yu. Murzin, Transformation of levoglucosan over H-MCM-22 zeolite and H-MCM-41 mesoporous molecular sieve catalysts. Biomass Bioenergy, doi:10.1016/j.biombioe.2011.01.046, in press.
[33] M. Käldström, N. Kumar, T. Heikkilä, M. Tiitta, T. Salmi, D.Yu. Murzin, ChemCatChem 2 (2010) 539–546.
[34] Z. Srokol, A.G. Bouche, A. Estrik, R.C.J. Strik, T. Maschmeyer, J.A. Peters, Carbohydr. Res. 339 (2004) 1717–1726.
[35] A. Aho, M. Käldström, P. Fardim, N. Kumar, K. Eränen, T. Salmi, B. Holmbom, M. Hupa, D.Yu. Murzin, Cell Chem. Technol. 44 (2010) 89–96.
[36] L. Smrčok, M. Sládkovičová, V. Langer, C.C. Wilson, M. Koóš, Acta Crystallogr. 62 (2006) 912–918.